International Journal of Science and Research (IJSR)
ISSN (Online): 2319-7064
Index Copernicus Value (2013): 6.14 | Impact Factor (2015): 6.391

AFM and Optical Study of Graphene Oxide and In_2S_3/GRO: Effect of Thickness

A. Timoumi*, M. K. AL Turkestani, J. Ouerfelli

Department of Physics, Faculty of Applied Sciences, Umm Al-Qura University, 21955 Makka, Saudi Arabia

*Corresponding author: E-mail: timoumiabdelmajid[at]yahoo.fr, Tel: 00 966 56 270 3945

Abstract: ***Continuous efforts have been done to develop high quality Graphene in large area for both research purposes and with a view to possible applications. Although most of the research progress has been made in understanding the structure, processing and properties of GRO/GRO-based compound, there is significantly more to be explored and exploited given the highly versatile physical properties of the material. In this work we report an efficient and easily accessible route to synthesize graphene oxide using modified Hummer's method, indium sulphide and In_2S_3-GRO composites by a hydrothermal process. The films were fabricated in various thicknesses, which allow studying the effect of the thickness on the material properties. Surface morphology of the samples was investigated using atomic force microscopy (AFM), which showed that films had a continuous coverage with a smooth surface. The optical characteristics of the deposited films were obtained from the analysis of the transmission and reflectance spectral data over the wavelength range of 300-1800 nm. The optical absorption data yielded a direct band gap energy of 3.4eV for GO sample, while the bad gap varies from 3.7 to 3.0 eV for the In_2S_3/GO-based samples depending on the thickness of the In_2S_3 itself. This work provides new insights into utilizing In_2S_3/GO composites for energy conversion.***

Keywords: Graphene oxide, Spin coating, Indium sulphide, Thickness

1. Introduction

Photovoltaic fields are attracting more and more attention because of their potential for solving environmental and energy problems, which are the biggest challenges of the 21st century. Thus, numerous attempts have been made on the fabrication of semiconductor nanomaterials as potential alternative photocatalysts with desirable visible light activities. Recently, graphene-based assemblies are gaining attention as a viable alternate route to boost the efficiency of photocatalysts. Graphene is a planar monolayer of carbon atoms that arrange into a two-dimensional lattice with sp^2 hybridized and a carbon-carbon bond length of 0.142 nm [1-5]. Graphene is a basic building block of graphitic materials for all dimensionalities.

To date, several Graphene-based composites have been reported for their improved photocatalytic properties. However, little attention has been given to In_2S_3/Graphene nanocomposites. Recent years have witnessed the flourish of constructing Graphene (GR)-semiconductor composite photocatalysts for conversion of solar energy [6-9] since the discovery of GR in 2004 [10]. Due to the remarkable physical and chemical properties of GR, various GR-based semiconductor have been designed and widely applied in a various fields such us; polymer nanocomposites, super-capacitor devices, drug delivery systems, solar cells [11], memory devices, transistor devices, biosensors and electromagnetic/microwave absorption shields. Recently, divers group reported the fabrication of GR-CdS [12], GR-TiO_2, and GR-ZnS nanocomposites and their application for aerobic selective oxidation of alcohols to aldehydes and oxidation of alkenes to peroxides under visible light illumination. In addition, the utilization of one dimensional CdS nanowires reduced graphene oxide (RGO) for selective reduction of nitro compounds under visible light irradiation is studied. However, CdS semiconductor often suffers from environmental problems due to the fact that cadmium (Cd) is toxic to most organisms and has been classified as carcinogenic and mutagenic. Thus, an alternative choice of GR-semiconductor composite photocatalysts with low toxicity would be more desirable and environmentally benign. Its large surface area, high carrier transport mobility, superior mechanical flexibility, and excellent thermal/chemical stability render it a promising alternative as an electron-accepting material for photovoltaic [13-19].

Many attempts have been done to make use of In_2S_3 as a visible light-driven photocatalyst for degradation of organic dyes, water splitting to hydrogen, dry cell and photocatalysis [20-26]. However, to the best of our knowledge, reports on In_2S_3-GR composites for photocatalytic selective redox reaction applications are relatively limited. In particular, application of In_2S_3/GR as a visible light-driven photocatalysts for selective reduction of nitroaromatic compounds remains unavailable so far. Against this background, where in report the synthesis of In_2S_3/GR nanocomposites via an efficient and a simple self-assembly approach during which the positively charged In_2S_3 is coupled with negatively charged Graphene oxide (GO) by the electrostatic attractive interaction. GO [27] is reduced to graphene by hydrothermal treatment. This work highlights the important synthesis and thickness effect of In_2S_3/GR semiconductor nanocomposites.

2. Experimental Details

Figure 1 shows the sample route for synthesis of GO and In_2S_3/GR thin layers.

Licensed Under Creative Commons Attribution CC BY

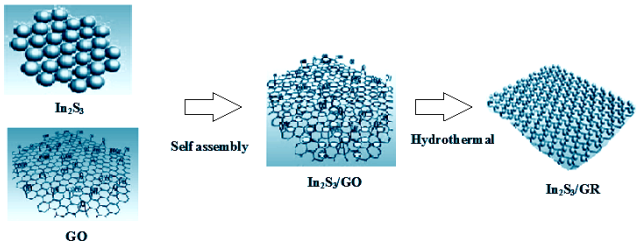

Graphene oxide was synthesized from flake graphite by a modified Hummers method. GO/In_2S_3 composites were synthesized by a one-step hydrothermal growth reaction. In a typical process, 5g of graphite fine powder with 5g of $NaNO_3$ were dissolved in 23 mL H_2SO_4 in ice bath with a constant stirring for 4h prior to adding 6.0 g $KMnO_4$. Next, 3 g of $KMnO_4$ and 46 ml of H_2O, were added to this solution. The mixture was stirred in a water bath for 120 min to get a homogeneous solution. After 120 min, 250 mL of desionized water was slowly added, and the temperature of the solution was raised to 98℃ for additional 60min. Then, the reaction was stopped by adding desionized water (250 mL) and H_2O_2 (10mL, 35%) during 1h. The solution's color transformed to brilliant yellow. In_2S_3 was added with constant stirring to obtain a homogeneous solution. In_2S_3/GO was spin coated on a glass substrate at 3000 rpm for 30s. Then, substrates was annealed at 250℃ for 60 min.

The Surface morphology was examined using Atomic Force Microscopy AFM; VeecoCP-II in contact mode with Si tips at a scan rate 1 Hz. Optical measurements were acquired at room temperature in the spectral range of 200-1800 nm by using a computer-aided double-beam spectrophotometer (Shimadzu 3150 UV-VIS-NIR) with a resolution of 0.1 nm.

3. Results and Discussion

3.3. AFM Analysis

Surface morphology was analyzed using atomic force microscopy (AFM). The 2D and 3D AFM images of the annealed composite films with various thicknesses presented in Figure 2.

The scanned surface area is 5µm×5µm. The AFM micrographs reveal the continuous coverage, of the layers and show that the film surface morphologies depend on the thickness. The root mean square (RMS) roughness value varies with thickness. This result could be explained by the agglomeration after annealing. The film growth proceeds through agglomeration of the islands. These islands later coalesce together to form the continuous film with further increase of temperature leading to homogeneous topography [28]. This can be related to the strong effect of the capillary forces on the surface of films. No principal change in the morphology is observed on the images of the films.

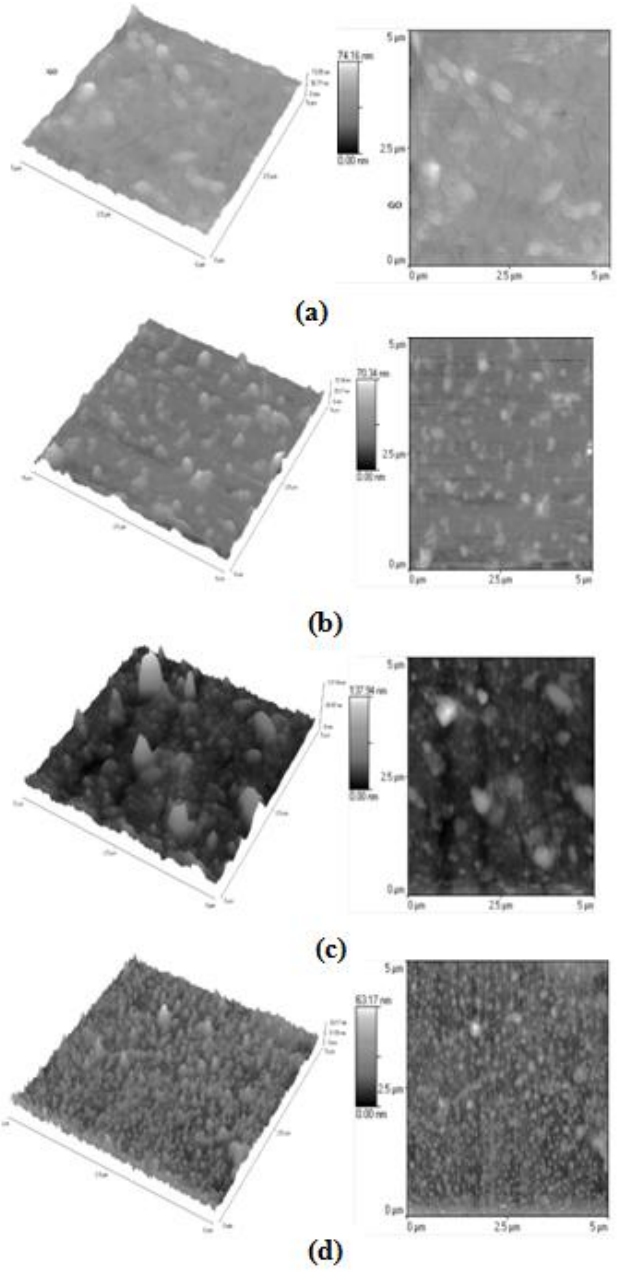

Figure 2: 2D and 3D AFM images In_2S_3/GR films with different thickness

Table I summarizes the roughness evaluated from AFM measurements as function of thickness layers. We note that Thermal annealing at 523K during 60 min produces the following changes in roughness.

Table 1: Roughness of annealed GO and In_2S_3/GO films with different thickness.

Samples	GO	In_2S_3/GO		
Thickness (nm)	150	200	250	300
Roughness (nm)	8.4	6.2	9.0	22.2

The grain size of the deposited films varied with the thickness, which may be attributed to the nucleation on the substrate. The root mean square (rms) roughness of the film increases with increasing thickness. The highest

Licensed Under Creative Commons Attribution CC BY

roughness is obtained from the film of greater roughness with 300 nm.

3.1: Optical Studies

Optical transmission measurements in the wavelength range 200-1800 nm were also performed in order to investigate the effect thickness on the optical performances of window layers. Figure 3 shows the optical transmittance of the films with various thicknesses deposited on glass substrates. All layers show good transmittance reaching 55 % in visible and 65 % in near-IR region.

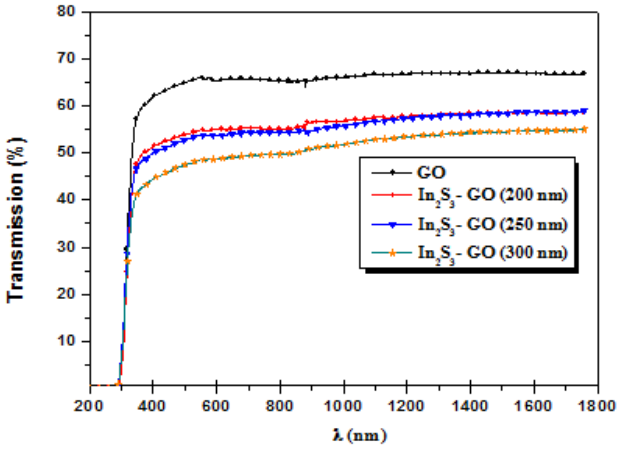

Figure 3: Optical transmittance of GO and In_2S_3/GR films with different thickness

The optical band gap of the films is determined by the following relation [29]:

$$(\alpha h\nu) = A(h\nu - E_g)^n$$

where A is a constant, Eg is the optical band gap and the exponent n characterizes the nature of band transition, α is the absorption coefficient, h is the Planck`s constant is and ν is the frequency.

Figure 4 shows the variation of $(\alpha h\nu)^2$ against hν. The band gap energy is determined by extrapolating the straight line portion to the energy basis at α = 0.

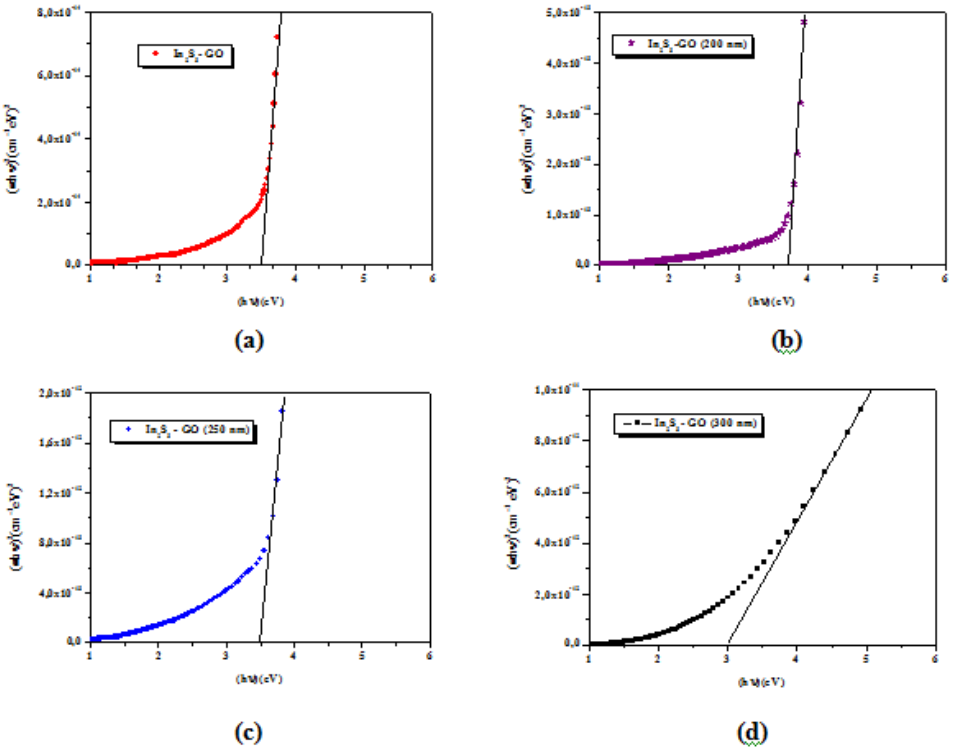

Figure 4: Tauc plot (i.e. $(\alpha h\nu)^2$vs hν) using UV-vies-NIR absorption spectra for as prepared (a) GO and In_2S_3/GO films of (b) 200, (c) 250 and (d) 300nm thickness, respectively

Licensed Under Creative Commons Attribution CC BY

We noticed that the gap energy has spent from 3.0 eV to 3.7 eV. It is remarkable that this variation is linear with the variation thickness. It is known that the optical characteristics of semiconducting thin films may vary with the thickness of these films. Such behavior may occur due to several reasons such as the variation in the stoichiometry of the films. A vacancy in the crystal structure of semiconductors is well known to create crystallographic defects, which form localized energy states in the band gap. This may affect the interaction between semiconductors and light, and therefore alters the band gap.

4. Conclusion

GO was synthesized using Hummers method and annealed at 573K for thermally reduced GO. In_2S_3/GO was synthesized and deposited on glass substrates using spin coating method. The surface morphology and optical properties of annealed GO and In_2S_3/GO thin film of different thickness have been studied. Studies using AFM indicates the formation of graphene oxide. The optical band gap Eg was found to be 3.4eV for GO while it varies from 3.7 to 3.0 eV with varying the In_2S_3/GO thickness.

Acknowledgment

The authors would like to thank King Abdulaziz City of Science and Technology (KACST) for the financial support (Project ID: 86-35).

References

[1] H. Wang, X. Yuan, Y. Wu, H. Huang, X. Peng, G. Zeng, H. Zhong, J. Liang, M. Ren, Adv. Colloid Interface Sci. 195-196 (2013) 19-40.
[2] A. Reina, X. Jia, J. Ho, D. Nezich, H. Son, V. Bulovic, M.S. Dresselhaus, J. Kong, Nano Lett. 9 (2009) 30-35.
[3] M. B. M. Krishna, N. Venkatramaiah, R. Venkatesan, D. N. Rao, J. Mater. Chem. 22 (2012) 3059-3068.
[4] Z. Sun, D.K. James, J.M. Tour, J. Phys. Chem. Lett. 2 (2011) 2425-2432.
[5] T. Kuila, S. Bose, A. K. Mishra, P. Khanra, N.H. Kim, J.H. Lee, Progr. Mater. Sci. 57 (2012) 1061-1105.
[6] K. H. Hung, C. H. Chan, H. W. Wang, Renewable Energy 66 (2014) 150-158.
[7] W.T. Wu, S.H. Yang, C.M. Hsu, W.T. Wu, Diamond and R. Materials, 65 (2016) 91-95.
[8] M. Lee, S. K. Balasingam, Y. Ko, H. Y. Jeong, B. K. Min, Y. J. Yun, Y. Jun, Synthetic Metals, Volume 215 (2016) 110-115.
[9] G. Wang, W. Xing, S. Zhuo, Electrochimica Acta 92 (2013) 269 - 275.
[10] K. S. Novoselov, A. K. Geim, S. V. Morozov, D. Jiang, Y. Zhang, S. V. Dubonos, I. V. Grigorieva, A. A. Firsov, Science 306 (2004) 666-669.
[11] Y. H. Hu, H. Wang, B. Hu, Chem. Sus. Chem 3 (2010) 782 - 796.
[12] C. H. Deng, J. L. Gong, G. M. Zeng, Y. Jiang, C. Zhang, H. Y. Liu, S. Y. Huan, Chemical Engineering Journal, 284 (2016) 41-53.
[13] D. S. Yu, Y. Yang, M. Durstock, J. B. Baek, L. M. Dai, ACS Nano 4 (2010) 5633-5640.
[14] Z. F. Liu, Q. Liu, Y. Huang, Y. F. Ma, S. G. Yin, X. Y. Zhang, W. Sun, Y. S. Chen, Advanced Materials 20 (2008) 3924-3930.
[15] Q. Liu, Z. F. Liu, X. Y. Zhang, N. Zhang, L. Y. Yang, S. G. Yin, Y. S. Chen, Applied Physics Letters 92 (2008) 223303-1-223303-3.
[16] Q. Liu, Z. F. Liu, X. Y. Zhang, L. Y. Yang, N. Zhang, G. L. Pan, S. G. Yin, Y. S. Chen, J. Wei, Advanced Functional Materials 19 (2008) 894-904.
[17] Z. Y. Liu, D. W. He, Y. S. Wang, H. P. Wu, J. G. Wang, Solar Energy Materials and Solar Cells 94 (2010) 1196-1200.
[18] Z. Y. Liu, D. W. He, Y. S. Wang ,H. P. Wu, J. G. Wang, H. T. Wang, Solar Energy Materials and Solar Cells 94 (2010) 2148-2153.
[19] C. M. Hill, Y. Zhu, S. L. Pan, ACS Nano 5 (2011) 942-951.
[20] A. Timoumi, H. Bouzouita, M. Kanzari, B. Rezig, Thin Solid Films, 480-481 (2005) 124-128.
[21] K. H. Park, K. Jang and S. Uk Son, Angew. Chem., Int. Ed., 45 (2006) 4608.
[22] W. Du, J. Zhu, S Li and X. Qian, Cryst. Growth Des., 8 (2008) 2130.
[23] Y. Xing, H. Zhang, S. Song, J. Feng, Y. Lei, L. Zhao, M. Li, Chem. Com., (2008) 1476.
[24] L. Chen, Z. Zhang and W. Wang, J. Phys. Chem. C, 112 (2008) 4117.
[25] A.M. Franzman and L. R. Brutchey, Chem. Mater., 21 (2009)1790.
[26] G. Liu, X. Jiao, Z. Qin and D. Chen, Cryst Eng. Comm, 13 (2011) 182.
[27] S. Park, J. An, I. Jung, R.D. Piner, S.J. An, X. Li, A. Velamakanni, R.S. Ruoff, Nano Lett. 9 (2009) 1593-1597.
[28] S. J. Ikhmayies, R.N. Ahmad-Bitar, Appl. Surf. Sci. 255 (2008) 2627.
[29] N. Pentyala, R. K. Guduru, E. M. Shnerpunas, P. S. Mohanty, Applied Surface Science, Vol. 257 (2011) 6850-6857

Licensed Under Creative Commons Attribution CC BY